XIV International Conference on Computational Plasticity. Fundamentals and Applications
COMPLAS XIV
E. Oñate, D.R.J. Owen, D. Peric & M. Chiumenti (Eds)

# FAST COMPUTATION: A STEADY-STATE SIMULATION OF RAILWAYS BALLASTED TRACK SETTLEMENT

**THIBAULT BADINIER[*,†], SIEGFRIED MAÏOLINO[*] AND HABIBOU MAÏTOURNAM[†]**

[*] Geological and Geotechnical Hazards Research Team
Cerema Centre Est, Département Laboratoire de Lyon
25 avenue François Mitterrand, 69500 Bron, France
web page: http://www.centre-est.cerema.fr

[†]Institut des Sciences de la Mécanique et Applications Industrielles (IMSIA; UMR 9219)
Unité de Mecanique (UME), ENSTA ParisTech
828 Boulevard des Maréchaux, 91120, France
Web page: http://www.imsia.cnrs.fr/

**Key words:** Computational Plasticity, Railway, Ballast, Geomaterials, Finites Elements Methods, Steady State

**Abstract.** Geometry of ballasted railways track is a major concern in railroads safety and efficiency. Settlement of railways ballast has been studied to help railway infrastructure managers to keep infrastructures in shape and to prevent accidents.

In this paper, we present an innovative numerical approach to study railways ballast settlement. Commonly used models representing a moving load need huge computation time. On the other hand, assuming static cyclic loading representation leads to discrepancies. Indeed, it does not conceder particularities of moving load. With this new model we want to avoid the drawbacks of previously developed methods.

We developed a steady state algorithm to compute plastic strain in geomaterials and to study behaviour of ballasted railways track with an Eulerian approach. This way we improved model efficiency by drastically reducing computation time while considering mobile load specificities.

## 1 INTRODUCTION

Railway tracks are usually composed of rails, sleepers and ballast. Rails support and guide the train, sleepers maintain rails and transmit load to the ballast, and ballast keeps sleepers in place, distributes load over the ground, and maintains all geometric aspects of the tracks. Geometry of tracks is a major concern in railways safety. A deviation of some millimetres with the normative prescription could lead to derailment and potential accidents.

In this paper we study railways settlement via a continuous approach, computing plastic strain in ballast layer under train traffic. The purpose of this paper is to evaluate the pros and cons of different numerical computational methods.

We chose to study impact of a moving load on the structure in opposition with other classical methods which use a static load, varying in sinusoidal cycles for example. Those simplified load cycle representations hides particular yielding condition due to load movement. This could lead to major discrepancies during computation.

We developed two different algorithms, using two different methods to represent load movement. First, a classical Step-by-Step method, representing movement with many small incremental displacements. And secondly, an innovative Steady-Sate method, using Eulerian assumption and representing continuous flow movement.

We tested both algorithm on the same railways model to be able to compare the results in the same conditions, especially the computation time.

## 2 RAILWAYS BALLAST BEHAVIOUR

Although ballast is composed of a multitude of smalls blocks, we focus on global behaviour. The ballast layers are modelled using a continuous materials assumptions and studied with Finites Element Methods (FEM) which is easier to implement and needs less computational time than Discrete Elements Methods (DEM). The continuous approach is useful to study structure deformation as an accumulation of plastic strain. This approach has already been used to study ballasted track in different works [1, 2, 3]

### 2.1 Elastic-Plastic behaviour

We suppose infinitesimal strain which means additive decomposition between elastic and plastic strain tensor (equation 1).

$$\underline{\underline{\varepsilon}} = \underline{\underline{\varepsilon}}^e + \underline{\underline{\varepsilon}}^p \tag{1}$$

Relation between elastic strain $\underline{\underline{\varepsilon}}^e$ and stress tensor $\underline{\underline{\sigma}}$ [1] are supposed to be isotropic linear elastic behaviour, described with Hooke's equation. Young's Modulus and Poisson coefficient are taken from Profillidis study [4], *i.e.* $E = 110\text{MPa}$ and $\nu = 0.2$.

Plastic strain $\underline{\underline{\varepsilon}}^p$ evolution is described using plastic criterion written as a yield function $f(\underline{\underline{\sigma}})$ ($f(\underline{\underline{\sigma}}) < 0$ stress state is acceptable ; $f(\underline{\underline{\sigma}}) = 0$ plastic strain can grow ; stress state is not acceptable $f(\underline{\underline{\sigma}}) > 0$). For simplification reason, we consider ballast with a "standard" bahaviour, *i.e.* flow rule is described as a gradient of the yield function :

$$\dot{\underline{\underline{\varepsilon}}}^p = \lambda \frac{\partial f(\underline{\underline{\sigma}})}{\partial \underline{\underline{\sigma}}} \tag{2}$$

1. **Sign convention** : Traction are positive, and principal stresses are ordered as follows : $\sigma_I \geq \sigma_{II} \geq \sigma_{III}$

### 2.2 Commonly used criteria

Geomaterial behaviour description commonly uses dedicated criteria such as the Mohr-Coulomb criterion, the Matsuoka-Nakai criterion[5] and the Drucker-Prager criterion[6] (Figure 1).

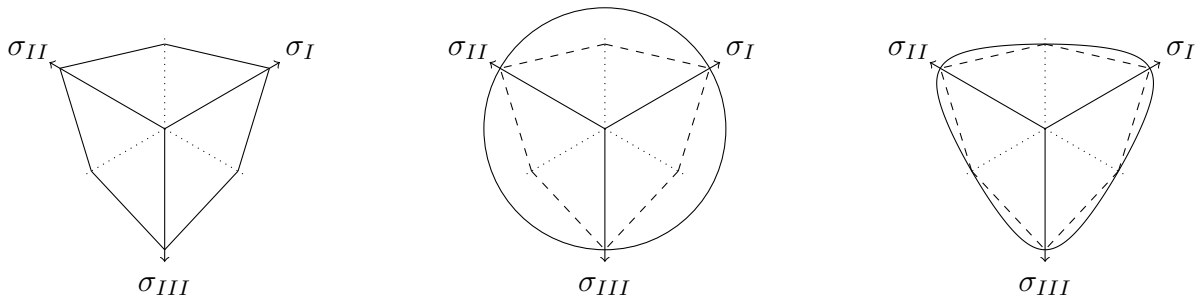


(a) Mohr-Coulomb criterion

(b) Drucker-Prager Criterion compression fitted on Mohr-Coulonb

(c) Matsuka-Nakain criterion fitted on Mohr-Coulomb

**Figure 1**: Commonly used Criteria represented din $Pi$-plane

The Mohr-Coulomb criterion is the most commonly used criterion in geo-technical engineering. Its parameters (cohesion $C$ and internal friction angle $\phi$) are easy to deduce from laboratory tests and meaningful for engineers. They are commonly used to describe material and Fitting parameter can be described to use other criterion

The Drucker-Prager criterion is the simplest geo-technical criterion, with a circular conical yield surface. It allow direct computation of plastic strain using radial return[7, 8].

The Matsuoka-Nakai criterion is a more complex criterion, with a smooth conical yield surface. It avoids angular problem during flow rule computation in opposition with Mohr-Coulomb . Moreover, this criterion seems to excellently fit to real tri-axial tests [5]. This criterion easily fits on Mohr-Coulomb (see figure 1(c)).

In previous works [9, 10, 11] we compared those three criteria. Firstly, Drucker-Prager improve computation speed of plastic strain. Secondly, despite its induced mist-estimated resistance of materials, a wisely chosen Drucker-Prager fitting keeps discrepancies to an acceptable level. For this reason we use the compression fitted Drucker-Prager criterion (figure 1(b)). We use yield function from equation (3) with mean stress $\sigma_m$ and deviatoric stress amplitude $J_2$. Fitting parameters are gives in equation (4).

For this study we will use $\phi = 40^\circ$ [12] and $C = 5\text{Pa}$ [2].

$$f(\underline{\underline{\sigma}}) = 3\alpha(\sigma_m - H) + \sqrt{J_2} \tag{3}$$

$$\alpha = \frac{2\sin\phi}{\sqrt{3}(3+\sin\phi)} \text{ and } H = \frac{C}{\tan\phi} \tag{4}$$

2. The ballast is supposed to be cohesion-less but we take a negligible $C$ value to avoid zero division issues during the computation process.

## 3 COMPUTATIONAL METHODS

Computation of $\underline{\underline{\varepsilon}}^p$ depends on stress path followed by particles during load cycle. Many classical cyclic loading models commonly use 2D or 3D structure with a static sinusoidal loading which induces increasing and decreasing stress path following a determined way. Mobile load, such as train on railways, induce a particular strain path witch has a major importance for plastic strain determination.

Here, we propose here two different methods to compute plastic strain under a mobile load.

For following part we will suppose that our structure is a $\vec{x}$ axial structure and the load move downstream on the structure. *i.e.* load speed is $\vec{V} = -V\vec{x}$, constant.

### 3.1 Step-by-Step Computation Methods and Algorithms

The step-by-step algorithm is a classical method to compute influence of a mobile load on a structure based on an incremental displacement of the load (see figure 3(a)).

We focus on a central part of the structure. Before loading cycle, initial plastic strain are taken from previous load passing or are induced by the weight of the structure itself. We start by locating the load before the considered section of the structure, on abscissa $X_0$, and we compute elastic-plastic strain state on the entire structure.

At time $t$ the structure is on a $\underline{\underline{\varepsilon}}^p_t$ plastic strain state, and abscissa of the load is $X_t$. At the next step, time is $t + \Delta t$, the load is now at abscissa $X_{t+\delta t} = X_t - V \cdot \delta t$ (see figure 3(a)). For the new configuration, we compute plastic strain $\underline{\underline{\varepsilon}}^p_{T+\delta t}$ taking account previous plastic strain $\underline{\underline{\varepsilon}}^p_t$. (Equation 5)

$$\underline{\underline{\varepsilon}}^p_{t+\delta t} = \underline{\underline{\varepsilon}}^p_t + \lambda \frac{\partial f(\underline{\underline{\sigma}})}{\partial \underline{\underline{\sigma}}} \tag{5}$$

On each Gauss point the plastic strain are searched by closest point projection process[13, 7] until stress state are acceptable. When stress-strain state for the time $t$ are validated, we move the load decreasing abscissa from $X_t$ to $X_{t+1}$.

The load moves this way from before to after the studied part of the structure on $T$ different steps. After the $T$ computation phases we stop the computational process and we consider that stress-strain state of the studied element (usually central elements) is representative of the global stress-strain state of the entire structure after the loading cycle.

This method is limited because of the non continuous loading of the structure. To ensure a correct stress path description we need to use small $\delta t$ steps which multiply the number of steps. Remembering that the entire strain state has to be computed on each step, computational time is also multiplied and can be huge.

### 3.2 Steady-State Computation

The steady-state is an Eulerian methods which allows stress-strain state computation of a structure under a moving load. This method is based on the works of Nguyen and

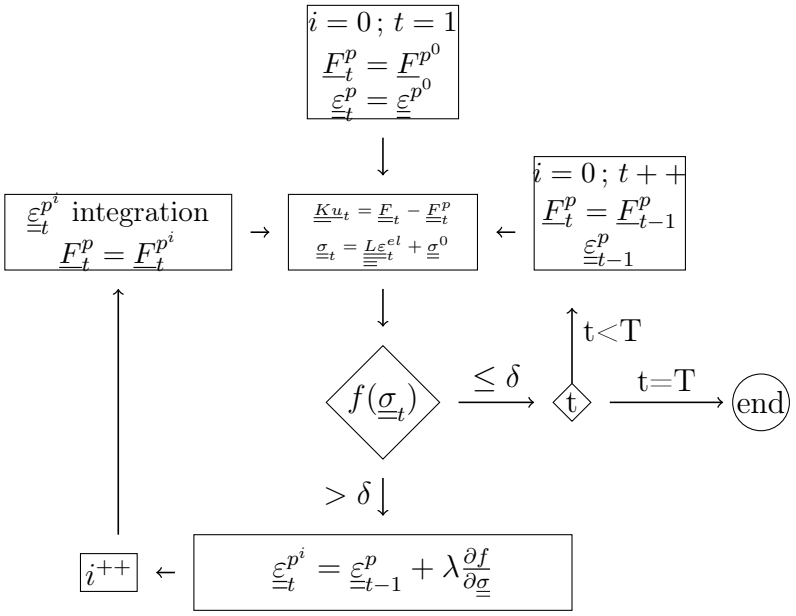


**Figure 2**: Step-By-Step Algorithm

Rahimian [14](1981) and Dang Van et al. [15](1985) who described the theoretical framework and first applications of the method. It has been used to various problems involving moving loads, such as the impact of rolling on rail heads [16], interaction between rock and cutting tool [17], automotive brake disk [18], tunnelling [19, 20]. But it as been never used to study ballast behaviour under train traffic.

### 3.2.1 Basic Concept

The method is based on a load point of view focus, the structure is then seen as material flow that goes under the load (see figure 3(b)). Primary, the method supposes that the structure is continuous and invariant along $\vec{x}$ axis. It also supposes that the load speed $\vec{V}$ and the load intensity are constant during a passage.

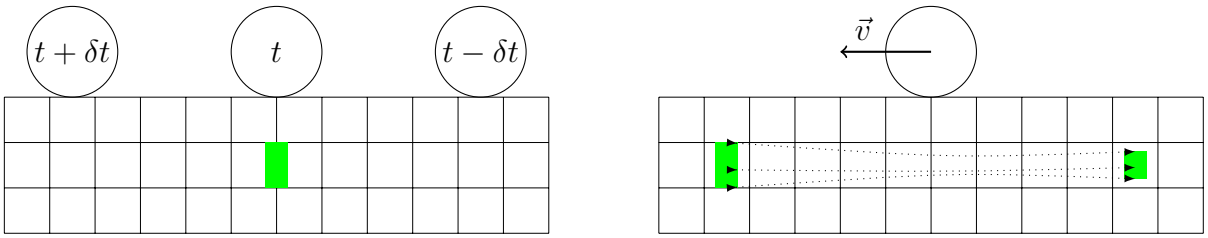


(a) Step-by-Step computation methods (b) Steady-State computational methods

**Figure 3**: Difference between Step-by-Step and Steady-State

It is possible to use a modified algorithm to compute non constant load or load at non constant speed. The TRC algorithm (Transitoire dans le Repère de Chargement)

developed by Nguyen-Tajan [21](2002) allows such particularities. In case of an periodic structure, such as railways tracks using sleepers, we can use another modified steady state algorithm. This particular aspect is not the purpose of this paper, it will be the subject of future work.

### 3.2.2 Computational Methods

Under a moving load the time derivative of a tonsorial quantity $\underline{\underline{A}}$ can be written as equation (6) from the structure point of view, and be rewritten as equation (7) from a load point of view.

$$\dot{\underline{\underline{A}}} = \frac{\partial \underline{\underline{A}}}{\partial t} + \vec{V} \cdot \vec{grad} \underline{\underline{A}} \tag{6}$$

$$\dot{\underline{\underline{A}}} = V \frac{\partial \underline{\underline{A}}}{\partial x} \tag{7}$$

In a steady-state method the plastic flow rules can be rewritten :

$$\dot{\underline{\underline{\varepsilon}}}^p = \lambda \frac{\partial f}{\partial \underline{\underline{\sigma}}} \tag{8}$$

With $\lambda \cdot f = 0$, $\lambda \cdot \dot{f} = 0$, $\lambda \geq 0$ and $f \leq 0$.

$$\frac{\partial \underline{\underline{\varepsilon}}^p}{\partial x} = \Lambda \frac{\partial f}{\partial \underline{\underline{\sigma}}} \tag{9}$$

With $\Lambda > 0$ if $f = 0$ and $\frac{\partial f}{\partial x} = 0$ or $\Lambda = 0$ otherwise.

Steady state methods consider that stress path during the loading cycle can be described by following the stress state on a line parallel to the structure axis. Plastic strain are then computed on the integrations points (Gauss points) which are lined because of quadrilateral mesh construction.

Gauss points are then noted and sorted on many parallels lines along the structure. To compute the plastic strain at point $n$ we use the plastic strain state on the previous Gauss point $n-1$, because we assume the continuous yielding during the movement (see figure 4). Equation (10) is used to compute the plastic strain in point $n$.

$$\underline{\underline{\varepsilon}}^p_n = \underline{\underline{\varepsilon}}^p_{n-1} + \Lambda \frac{\partial f}{\partial \underline{\underline{\sigma}}} \tag{10}$$

### 3.2.3 Steady-State Algorithm

For the steady state algorithm we consider a central load over the structure that does not move. Before the loading cycle, initial plastic strain are taken from the previous load passes or are those induced by the weight of the structure itself.

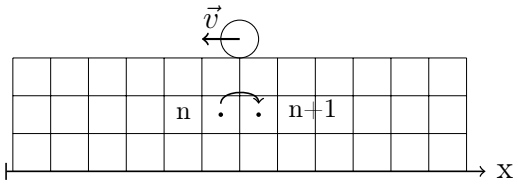


**Figure 4**: Plastic strain computation process on Gauss point

The plastic strain are then computed and integrated along each of Gauss points line flowing the particular computation process of Steady-State algorithm. The plastic strain are searched by the closest point projection process [13, 7] until stress state are acceptable all along the line. If it's not, the plastic strain integration is started over on the entire line.

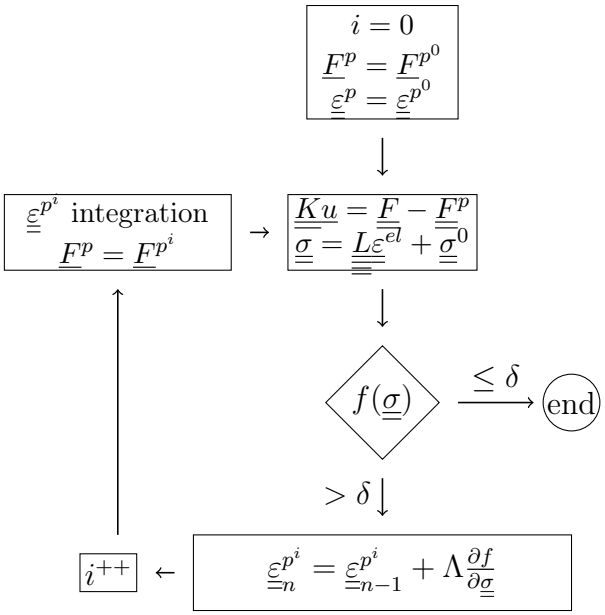


**Figure 5**: Steady-State Algorithm

At the end of the process, *i.e.* when stress state is acceptable on the entire structure, we identify the final plastic strain at the end of the structure, we consider that this stress-strain state is representative of the global stress-strain state of the entire structure.

For a multi-cycle loading computation, the process is repeated $N$ times for the $N$ loading cycles needed.

## 4 RAILWAYS MODELLING

We will illustrate the different computation methods using a 3D model of a Railways track. The Model is build in COMSOL Multiphysics FEM software and the computation is led with a Matlab routine. The two softwares communicated using Matlab LiveLink tools of COMSOL's software.

### 4.1 3D Model

The 3D model represent half of a symmetric 15m long railways track. The 2D transversal shape represent a 50cm hight ballast layers. Over it, a 25cm height and 1.1m wide half single block sleeper is disposed. On the side a 50cm shoulders, and die down slope with a 2/3 ratio are made. (See figure 6)

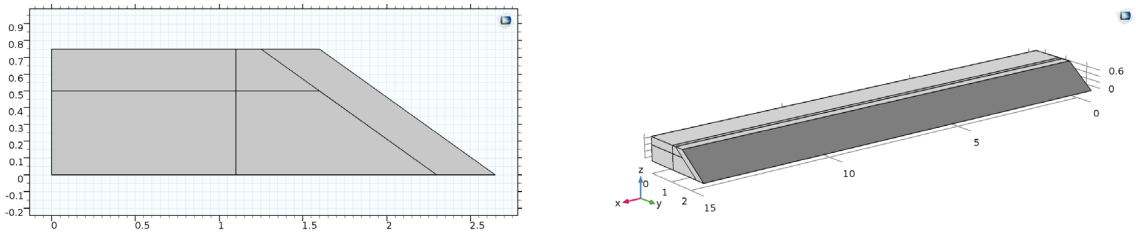

(a) 2D transversal shape (b) Full model

**Figure 6**: 3D Model of half a railway track

We focus on plastic strain under the sleepers, *i.e.* only in the 50cm bottom layer. Plastic strain are not significant in the rest of the structure and are not computed.

### 4.2 Meshing

The meshing use quadrilateral elements along the structure. The elements are built lined due to the steady-state computation assumption. Mesh element has to be smaller near the load to correctly describe stress repartition. Because the structure can be loaded on multiple spots, the Step-by-step model uses equally dense mesh. The Steady-state model uses a gradually dense mesh, denser in the middle of the structure, to limit the number of elements and improve computation time. Here we use three time fewer elements.

### 4.3 Load

Before any loading, the structure stability is computed supporting its own weight. The gravity will continue to affect the entire structure during all computation.

For this work the main load will correspond to a classical maximal load for our half track model. Because our model does not feature rail or sleepers, we will use an equivalent load continuously applied on the top of the bottom layers of ballast. The load repartition is taken from Profillidis work [4], and is interpolated to build a continuous loading (see figure 7). The total load is 10t, (20t for full axle load).

The load is placed on the middle of the structure for the Steady-State computed model, or can be moved along the structure with a parametrised position for the Step-by-Step de computed model.

For the Step-by-Step method we describe 57 steps equally distant from 20cm to ensure load zone covering step after step.

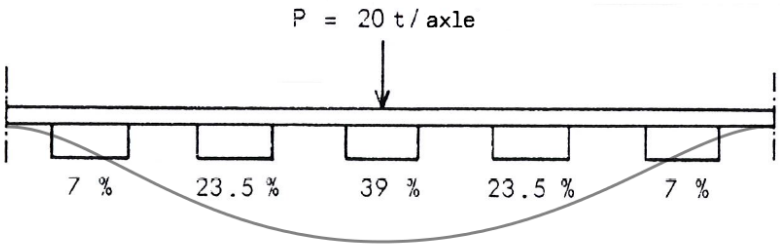


**Figure 7**: Load reparation on sleepers [4]

## 5 RESULT AND DISCUSSION

In the following part we will plot and compare plastic strain magnitude define as $\boldsymbol{\epsilon}^p = Tr(\underline{\underline{\varepsilon}}^p \cdot \underline{\underline{\varepsilon}}^p)$. Comparison of other measure of plastic strain has led to same conclusion and will not be presented.

### 5.1 Longitudinal representation

On figure 8, we represent plastic strain magnitude in the centre of a longitudinal slice of the model, for the Steady-State method and for the last steps of the Step-by-Step method. Those representations give us information on computation process accuracy and plastic strain distribution.

The steady-state algorithm figure shows plastic strain evolution from before to after the load passing. It also shows perfectly a regular and continuous plastic strain distribution after the load.

In opposition the step-by-step figure does not show us plastic strain evolution. To do so, we have to study plastic strain repartition on each step of the computation process. It also shows us an irregular and not continuous repartition of plastic strain. This is due to the jumping representation of load movement. The irregularities are not critical for the study but show a limitation of this methods.

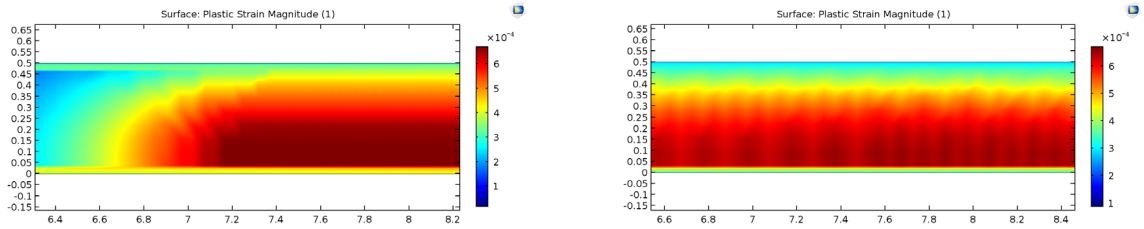


(a) Steady-State (b) Step-by-Step

**Figure 8**: Longitudinal repartition of plastic Strain for both methods

### 5.2 Transversal representation

On figure 9, we represent the transversal repartition of plastic strain magnitude in the representatives zones. Shape of the figure and measured values of plastic strain are totally comparable. For example, maximal magnitudes are $\boldsymbol{\varepsilon}^p = 6.76E^{-4}$ for steady-state and $\boldsymbol{\varepsilon}^p = 6.52E^{-4}$ for step-by-step, *i.e.* less than 5% discrepancies.

Both methods can be used to study plastic strain in railway ballast under train load. Small advantage for the Steady-State method who provide cleaner results and more informations.

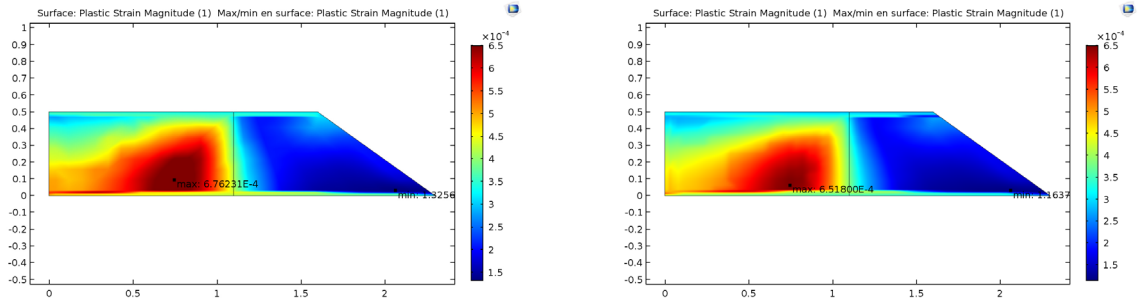


(a) Steady-State (b) Step-by-Step

**Figure 9**: Longitudinal repartition of plastic Strain for both methods

### 5.3 Computation time

For this model the step-by-step computation process had run for $395015s$ ($4d$, $13h$ and $43min$), the steady-state had run for $1940s$ ($32min$) [3]. This huge difference remain logical and can be explained as follow :

On one hand, the steady-state process correspond to a single full computation step of 24 iterations and both iteration takes about $80s$.

On the other hand, the step-by-step process correspond to 57 full computation steps. Each step needs about 24 iterations and each iteration takes about $260s$.

Those number are logical, by construction the Step-by-Step needs the same amount of computation on each steps as a full steady-state. Moreover, because of the 3 times denser meshing each iteration of a Step-by-Step need 3 times more time than a Steady-State iteration.

The same result was found with other tested model, independently from the different models and parameters.

Finally, the comparison of the computational time give a huge advantage to the Steady-State process over the Step-by-Step process.

3. These numbers may vary depending on the software and the computer, there are given to illustrate the comparison using same tools and conditions.

## 6 CONCLUSIONS

In this paper we studied possibilities of using the Steady-State computational methods for studying ballasted track settlement with a continuous approach. Considering the major importance of accurate moving load representation, we have looked for plastic strain computation methods under train circulation.

In that purpose we developed two algorithms using COMSOL Multiphysics and Livelink for Matlab. The first algorithm uses a classical computational method, Step-By-step methods, based on the movement representation via multiples small incremental displacements. The second algorithm uses an innovative Eulerian method, the Seady-State method, based on a load centred point of view and assuring the continuous yielding of the structure.

Using and comparing both methods showed minor differences between the results, with a small advantage for the Steady-State methods which provide homogeneous result. More importantly, comparing computational times showed a strong advantage for Eulerian method over the incremental method with a drastic computation time reducing, which let us see great potential for the Steady-State algorithms. Moreover, because our examples and models are quite simple, this advantage could be even more important for more complex model, including viscous-plastic behaviour for example.

The Steady-State algorithm give us many others potential advantage, including precise plastic strain and plastic work study during cycle, or cyclic structure study. Those improvements will be subject of further work and development in near future.

## RÉFÉRENCES

[1] Profillidis, V. *La voie ferrée et sa fondation - Modélisation mathématique.* Theses, Ecole nationale des ponts et chaussées - ENPC (1983). URL `https://pastel.archives-ouvertes.fr/pastel-00693511`.

[2] Suiker, A. *The mechanical behavior of ballasted railway tracks (DUP Science).* Ph.D. thesis, PhD Thesis, Technische Universiteit Delft (2002).

[3] Paderno, C. *Comportement du ballast sous l'action du bourrage et du trafic ferroviaire.* Ph.D. thesis (2010).

[4] Profillidis, V. and Humbert, P. Étude en élastoplasticité par la méthode des éléments finis du comportement de la voie ferrée et de sa fondation. *Bulletin Liaison du Laboratoire des Ponts et Chaussées* **141** (1986).

[5] Matsuoka, H. and Nakai, T. Stress-deformation and strength characteristics of soil under three different principal stresses. In *Proc. JSCE*, vol. 232, 59–70 (1974).

[6] Drucker, D. C. and Prager, W. Soil mechanics and plastic analysis or limit design. *Quarterly of applied mathematics* **10** (1952).

[7] Krieg, R. and Key, S. Implementation of a time independent plasticity theory into structural computer programs. *Constitutive equations in viscoplasticity : Computational and engineering aspects* 125–137 (1976).

[8] Wilkins, J. L. Calculation of Elastic-plastic Flow. *Methods of Compuational Physics* **8** (1964).

[9] Maiolino, S. and Luong, M. P. Measuring discrepancies between coulomb and other geotechnical criteria : Drucker–prager and matsuoka–nakai. In *7th Euromech solid mechanics conference, Lisbon, Portugal*, 09–07 (2009).

[10] Badinier, T. and Maïolino, S. Computation of ballasted track damage : A comparison of Coulomb, Drucker Prager and Matsuoka Nakai criteria. In Pombo, J. (ed.) *The Third International Conference on Railway Technology : Research, Development and Maintenance* (Civil-Comp Press, 2016). URL `http://dx.doi.org/10.4203/ccp.110.21`. Paper 21.

[11] Badinier, T. and Maïolino, S. Limiting discrepancies in substitution of Mohr-Coulomb with fast computation smooth criteria : Application to ballast layer (Submitted).

[12] Suiker, A. S., Selig, E. T. and Frenkel, R. Static and cyclic triaxial testing of ballast and subballast. *Journal of geotechnical and geoenvironmental engineering* **131**, 771–782 (2005).

[13] Simo, J. and Hughes, T. J. Computational inelasticity, volume 7 of interdisciplinary applied mathematics (1998).

[14] Nguyen, Q. S. and Rahimian, M. Mouvement permanent d'une fissure en milieu élasto-plastique. *Journal de Mécanique appliquée* **5**, 95–120 (1981).

[15] Van, K. D., Inglebert, G. and PROIX, J. Sur un nouvel algorithme de calcul de structure élastoplastique en régime stationnaire. In *3ème Colloque :" Tendances actuelles en calcul de structures", Bastia* (1985).

[16] Maitournam, H. *Résolution numérique des problèmes élastoplastiques stationnaires.* Ph.D. thesis, Thèse de Doctorat de l'ENPC (1989).

[17] Geoffroy, H. *Etude de l'interaction roche/outil de forage : influence de l'usure sur les paramètres de coupe.* Ph.D. thesis (1996).

[18] Nguyen-Tajan, M.-L., Maitournam, H. and Thomas, J.-J. Une méthode de calcul de structures soumises à des chargements mobiles : Application au freinage automobile. *Revue Européenne des Eléments* **11**, 247–261 (2002).

[19] Corbetta, F. *Nouvelles méthodes d'étude des tunnels profonds : calculs analytiques et numériques.* Ph.D. thesis, EMP (1990).

[20] Maiolino, S. *Fonction de charge générale en géomécanique : application aux travaux souterrains.* Ph.D. thesis, Ecole Polytechnique X (2006).

[21] Nguyen-Tajan, T. M.-L. *Modélisation thermomécanique des disques de frein par une approche eulérienne.* Ph.D. thesis, Ecole Polytechnique X (2002).